FINAL REPORT

ON

AN INTEGRATED AERODYNAMIC/PROPULSION STUDY FOR GENERIC AERO-SPACE PLANES BASED ON WAVERIDER CONCEPTS

NASA Grant NAG-1-886

August 1991

G. Emanuel and M.L. Rasmussen
University of Oklahoma
School of Aerospace and Mechanical Engineering

I. INTRODUCTION

The design of trans-atmospheric vehicles, or aero-space planes as they have come to be known, places excruciating demands on present-day technology. These vehicles embrace the various requirements for space-transportation systems, civil transports, and military aircraft. They are envisaged to take off from a runway, accelerate to orbital speed, and then descent and land in a conventional manner. The Mach-number range would be from 0 to 25. The aero-space plane must provide sustained hypersonic flight in the altitude range from 80,000 to 150,000 feet. In addition to atmospheric maneuverability, it must also provide for efficient orbital changes.

Recent progress in the aerodynamic design of high-speed aircraft has recognized the need for the blending of wings, bodies and propulsion units. The calculation of the flow field and aerodynamics of such blended bodies is not accurately done by the semi-empirical merging of the calculations for the separate parts. Thus elaborate computer codes are used for the prediction of the flows involved. In many respects these codes are still in the developmental stages and are expensive and unsuitable for many design studies. they are used to best advantage when guided by a simplified analysis that has first shown the direction for optimizing an aero-space plane.

The objective of this NASA grant is to provide a unified aero-space plane analysis based on waverider technology. The project is thus concerned with the overall aerodynamic design and performance

of an aero-space plane. The vehicle is divided into three parts: a forebody, a scramjet, and an afterbody.

II. SUMMARY OF RESEARCH EFFORT

BY M.L. RASMUSSEN

1. Viscous effects on the forebodies of cone-derived waverider configurations have been studied. A simple means for determining the average skin-friction coefficient of laminar boundary layers has been established. This has been incorporated into a computer program that provides lift and drag coefficients and L/D for on-design waveriders when the wall temperature and Reynolds number based on length are specified. A wide range of waverider shapes for arbitrary Mach numbers can be studied. This analysis has been published as AME Research Report No. OU-AME-89-4, May 1989, which is a modified version of the M.S. thesis by Mr. William Martin.
2. A simplified version of the work described in item 1 was prepared for a paper presented of the 1st International Hypersonic Waverider Symposium at the University of Maryland in October 1990.[1] The simplification amounted to setting Pr = 1 and using a linear viscosity-temperature relation. The simplified results more readily portray the pertinent factors that govern the wide parametric study that was carried out.
3. A significant effort was made to carry out PNS calculations for cone-derived waveriders using a code due to Lawrence. In the viscous mode, stability problems associated with the sharp leading edges of the waveriders were insurmountable. On the

other hand, when the viscous terms were turned off, that is, in the Euler mode, computations for elliptic cone-derived waveriders could be carried out for a wide range of on-design and off-design situations. Many features of these computations turned out to be very interesting. Especially at the off-design conditions, due both to Mach number and orientation changes, a number of interesting shock patterns near the sharp leading edges were observed. These results were used for the Ph.D. dissertation of B.-H. Yoon, and they appear in the AME Research Report No. OU-AME-91-2, January 1991.[2] This work is continuing for the round-nosed waveriders associated with axisymmetric conical flow. The round-nosed waveriders are more difficult for the Lawrence code to handle because this code is based on a starting procedure associated with almost conical bodies. Although some progress has been made, this work is not complete. It is the basis of the Ph.D. research by Mr. Xiaohai He and will be continued without grant support.

4. The aforementioned research has been documented in the mentioned references, which have already been forwarded to NASA when they appeared. The following work dealing with power-law derived waveriders is new and has not been documented elsewhere. It is thus presented here in some detail. This work has been performed by Mr. Brad Duncan, a junior in Aerospace and Mechanical Engineering at O.U. Part of this work was presented at the Midwest Regional Papers Contest for ASME by Mr. Duncan, and it won overall *First*

Place. It will also be presented at the follow-on National Contest at the Winter Annual ASME Meeting.

5. Waveriders Derived from Power-Law Shocks

5.1 **Background.** Waveriders derived from flows past cones will lose some of their overall advantages when viscous-interaction effects are large, that is, when $M_\infty^3/Re^{1/2}$ becomes sufficiently large. For cones in the hypersonic limit $M_\infty \to \infty$, the shock lies very close to the body and, for ordinary ranges of Reynolds numbers, the shock layer cannot be delineated clearly into separate inviscid and viscous parts. Some of the problems associated with such strong viscous interactions can be brought to the fore by considering flow fields downstream of power-law shocks.

Consider the flow field generated downstream of a power-law shock in either planar ($\sigma=0$) or axisymmetric flow ($\sigma=1$) described by

$$R_s(x) = Cx^m ,$$

where C is a constant, and the index m is a constant less than or equal to unity (see Fig. 1). It is well known in hypersonic-flow theory that, when $M_\infty=\infty$, the flow field is self-similar and the body that supports the shock is a power-law body having the form

$$R_b(x) = C\eta_b x^m ,$$

where the factor $\eta_b \equiv R_b/R_s$ is a function of m, as shown in Fig. 2. The body-shape factor η_b vanishes when $m=2/(3+\sigma)$, which is the limit of blast-wave theory.

Figure 3 shows a comparison of an axisymmetric body and shock shapes for different values of m. All the body shapes have the same ratio of base radius to body length. For the cone (m=1), the shock lies very close to the body. As the value of the index m decreases, the shock lies relatively farther away from the body, that is, the shock-layer thickness becomes greater. Conceivably, therefore, bodies with thicker shock layers should be more suitable for utilizing air-breathing propulsion units since there is more room for the inlet and cowl to be positioned in the shock layer, and a larger mass flow rate of air in the shock layer can be accommodated.

The flow across the shock layer is not as uniform as it is for the cone, and the flow is expanding owing to the convex longitudinal curvature of the body shape. Figures 4a and 4b show the pressure profiles $P(\eta)/P(1)$ and the density profiles $Q(\eta)/Q(1)$ across the shock layer for the axisymmetric power-law shapes, where $\eta \equiv y/R_s(x)$ is the similarity variable. For m near 1/2, the pressure is

nearly constant in a large layer near the body (the entropy wake) and varies rapidly outside this layer towards the shock. The density is zero on the body in this approximation (for $m \neq 1$) and very small in the entropy-wake region near the power-law body. For m near 1/2, most of the mass flow is in a layer adjacent to the shock. Correspondingly, the temperature in the entropy-wake layer near the body is very high. This has important implications regarding the heat transfer. Thus, there are both favorable and unfavorable aspects of hypersonic flows associated with power-law shocks.

5.2 **Associated Waveriders.** Our purpose is to study the features of waveriders that are derived from the flows downstream of power-law shocks, especially as they relate to incorporating inlets within the shock layer. We are aware of only two previous works that pertain to waveriders generated by power-law shocks. The first is that of Cole and Zien.[3] They were concerned with finding optimum lift-to-drag ratios with viscous drag neglected. The second is that of Corda and Anderson[4] who searched for waverider shapes having a maximum L/D when viscous drag was taken into account. The goals of our study are different. We wish to describe the types of waverider shapes that can be obtained in a broad sense. There are many types of constraints that may be placed on the design of a hypersonic aircraft, and different constraints will produce different answers. For a

vehicle that is going into orbit, having a large lift may not be the most important factor in a design when other factors have competing roles. Thus, we wish to perform a parametric study that produces a catalog of different forebody shapes together with their associated aerodynamics.

In addition, and perhaps equally important, we wish to describe the nature of the shock-layer flow fields that are associated with waverider shapes. To the extent that this was done at all in the aforementioned references, it was done only incidentally. For our purposes, however, it is very germane since we are also interested in placing inlets in the shock layer. The heat-transfer properties will also be of prime interest.

We have at our disposal a tool that represents a major advantage in carrying out parametric studies. We have developed an approximate analytic solution to the flow field generated by a power-law shock that is very accurate. This enables us to describe streamlines, stream surfaces, and the shock-layer pressure, density, and velocity profiles in analytical form. Besides being beneficial to future users, it is beneficial to us because it allows us to see the inter-relationships of the different variables involved that are not readily apparent when elaborate numerical computations are

necessary.

5.3 **Construction of Waverider Shapes.** We briefly describe how waveriders are to be constructed by knowing the flow field downstream of a power-law shock. Figure 5 shows the top half of an axisymmetric flow through a power-law shock, and a typical streamline that starts at x_s at the shock. The lower half of the figure shows the same view reflected about the axis of symmetry but with a streamline from the freestream passing through the location x_s to form an upper freestream surface. The original streamline in the shock layer now forms a curved compression surface. This lower view constitutes a cross section of a waverider in the symmetric pitch plane. The thickness of the shock layer is greater than would be obtained for the corresponding flow past a cone (m=1).

Recall that the density profile across the shock layer of a power-law body has a significantly larger inviscid variation than in the shock layer of a cone, where the density is often approximated as a constant. In the power-law case, the density is largest near the shock and decreases to a small value at the body. As indicated in Figs. 3 and 5, our design procedure utilizes the higher density flow near the shock. An important consequence is that there is an increase in the air mass flow rate for the inlet relative to a comparable cone-derived forebody.

Figure 6 shows a perspective view from the rear of a power-law generated waverider. The compression surface and the shock attached to the lip, in general, have convex longitudinal curvatures. The design of the waverider would begin by specifying the trailing-edge curve in the base plane, which is analogous to the procedure used in the present grant and in our previous research. This fixes the shape of the top freestream surface, and then the compression surface can be determined analytically since the shock-layer streamlines are known in analytic form. Since the flow is axisymmetric, all the streamlines in the shock layer lie in planes that pass through the axis of symmetry of the basic power-law body, as shown in the figure. The lift, drag, pitching moment, volume, planform area, and so forth are all evaluated by surface integrals over the shock layer in the base plane, again analogous to our previous research. The entire analysis is carried out within the framework of hypersonic small-disturbance theory.

Besides the general shapes described above, there is also the special limiting shape that we refer to as the idealized power-law waverider. This idealized configuration is shown in Fig. 7. For this limiting case C_L/τ_b , C_L/τ_b^2 , and $\tau_b L/D$ depend only on the power-law index m, the anhedral angle ϕ_ℓ , and $\gamma \equiv C_p/C_v$. The

slenderness ratio of the basic body is denoted by $\tau_b = R_b/\ell$. The reference area is taken to be the base area.

The drag coefficient C_D/τ_b^2 is plotted versus m for $\gamma=1.4$ in Fig. 8a. It is independent of ϕ_ℓ since the reference area is the base area. As is well known from the theory for axisymmetric bodies, the minimum value occurs when $m\simeq0.7$. When $m\simeq0.58$, the drag is about the same as for the cone-derived waverider (m=1) for the same value of τ_b, but the shock layer is considerably thicker.

Figure 8b shows C_L/τ_b plotted versus m for several values of ϕ_ℓ. There is a minimum value when m is slightly less than 0.7.

Figure 8c shows the lift-to-drag ratio $\tau_b L/D$ plotted versus m for various values of ϕ_ℓ and $\gamma=1.4$. Both the lift and drag have minimums, but the minimum for the drag is deeper, and thus the ratio $\tau_b L/D$ has a maximum that occurs when m is slightly greater than 0.7. This type of behavior has been observed elsewhere in terms of longitudinal curvature effects.[5] Thus power-law derived waveriders can produce somewhat larger values of L/D, for the same value of τ_b, than cone-derived waveriders (m=1). In addition, the shock stands off farther from the body for the power-law derived waveriders.

Many types of shapes can be obtained from power-law derived waveriders, analogous to the many shapes obtained for the cone-derived waveriders in Ref. 1. Figure 9 shows $\tau_b L/D$ for waveriders with a parabolic top. The new parameter is $R_o \equiv (k/\eta_b) \cos \phi_\ell$, where k is measured as a percent of the base in the symmetry plane. The factor R_o is the normalized distance of the top surface in the base plane measured downward from the original axis of symmetry. These waveriders have the general shape shown in Fig. 6. When k=100%, the top freestream surface is flat. For these waveriders, the maximum value of $\tau_b L/D$ occurs when $m \simeq 0.64$. Compared to the cone-derived waveriders (m=1), a significant increase in L/D can be obtained and the shock stands off farther from the body, which is favorable for inlet design. Figure 10 shows another plot for the parabolic-top waveriders with $\phi_\ell = 60^\circ$ held fixed and k varied.

Figure 11 shows $\tau_b L/D$ for more generally shaped waveriders compared to the parabolic-top waveriders. Some improvement can be obtained in L/D, and other variations in shape conducive to winglets and control surfaces can be obtained.

An elaboration of these results will be presented by Mr. Brad Duncan at the 1991 ASME Winter Annual Meeting Undergraduate Papers Competition. The results are also

being prepared in the form of a paper for journal publication.

III. SUMMARY OF RESEARCH EFFORT

BY G. EMANUEL

We summarize Professor Emanuel's work and indicate those projects that are continuing even though NASA financial support is not available.

1. G. Emanuel, "A First Scramject Study," NASA CR 184965, Apr. 1989.

This report documents a variety of related scramjet engine topics in which primary emphasis is on simplicity and conceptual clarity. Thus, the flow is assumed to be one dimensional, the gas is thermally and calorically perfect, and the study focuses on low hypersonic Mach numbers. The first technical section evaluates the thrust and lift of an exposed half nozzle, which is used on the aero-space plane, as well as one that is fully confined. A rough estimate is provided of the drag of an aero-space plane. Background material dealing with thermal effects and shock waves is discussed in the next section. The following section then presents a parametric scramjet model, based on the influence coefficient method, that evaluates dominant scramjet processes. The independent parameters are the ratio of specific heats, a nondimensional heat addition parameter, and four Mach numbers. The total thrust generated by the combustor and nozzle is shown to be independent of the heat release distribution and the combuster exit Mach number, providing thermal choking is avoided. An operating condition for the combustor is found that maximizes the thrust. An alternative condition is explored when this optimum is no longer

realistic. This condition provides a favorable pressure gradient and a reasonable area ratio for the combustor. The next section provides parametric results based on the model. One significant finding is the sensitivity of the thrust to the value of the ratio of specific heats for the air upstream of the combuster. The final section summarizes and discusses the analysis.

2. Y.-Y. Bae and G. Emanuel, "Performance of an Aerospace Plane Propulsion Nozzle," J. Aircraft 28, 113-122, 1991.

A novel inviscid and viscous analysis is provided for a nozzle that is used with a scramjet for thrust generation. The analysis is based on the theory of a two-dimensional minimum length nozzle with a curved inlet surface, where the flow is sonic or supersonic. Inlet conditions are prescribed and the gas is assumed to be perfect. Viscous and inviscid nondimensional parametric results are provided for the thrust, lift, heat transfer, pitching moment, and a variety of boundary-layer thicknesses. In addition to global results, wall distributions of thrust, heat transfer, etc., are provided. The analysis demonstrates that the nozzle produces a lift force whose magnitude may exceed the thrust and a significant pitching moment. The thrust is sensitive to the inlet Mach number; it rapidly decreases as this Mach number increases. There is little loss in the thrust as the nozzle's downstream wall is truncated while the corresponding decrease in lift and pitching moment is moderate.

3. H.-K. Park and G. Emanuel, "Idealized Tip-to-Tail Waverider

Model," First Int. Hyp. Waverider Sym., Univ. of Maryland, Oct. 1990. See item 4 for a discussion of this work.

4. H.-K. Park and G. Emanuel, "Model of an Aero-Space Plane Based on an Idealized Cone-Derived Waverider Forebody," Research Rept. OU-AME-91-1, 1991, This report documents the code used in item 3.

The flow field for an idealized cone-derived waverider is axisymmetric. This feature is preserved for the rest of the vehicle including the inlet, cowl, combustor, and nozzle. We thus have a tip-to-tail model in which both the external and internal flows are axisymmetric. The assumption of axial symmetry provides a major simplification for the analysis and allows for a systematic integration of the propulsion unit with the aerodynamics. A novel design concept is used for the nozzle that avoids shock waves, minimizes the nozzle length, and tends to maximize its thrust.

The model is designed to provide lift, thrust, drag, and fuel consumption data for a vehicle cruising at a hypersonic Mach number. This is an initial formulation designed to provide only the most basic engineering data. Despite its idealized, inviscid limitations, it provides a self-consistent representation of both the aerodynamics and the scramjet/nozzle powerplant of the vehicle in a fully integrated configuration. In addition to describing the model, a range of parametric studies are presented. These studies yield dominant trends that can become the basis for more detailed studies.

The overall code is large and complex and its development has consumed almost two years of constant effort. This report

previously appeared as the Ph.D. dissertation of H.-K. Park. A listing of the code and a sample case is available on a 5" floppy disk by writing to G. Emanuel, University of Oklahoma, 865 Asp, Norman, Oklahoma 73019-0601.

5. G. Emanuel and C.-H. Hsu, "Lift and Drag of an Idealized Configuration in Supersonic Flight." In preparation for journal publication. A generalization of this effort with a different graduate student is in progress and will continue after the grant terminates.

The momentum theorem is utilized with different control surfaces to evaluate the lift and drag of an idealized configuration that conceptually represents an aero-space plane. The flow is assumed to be steady, inviscid, supersonic, two-dimensional, and without a combustion process. One objective is to discuss how the theorem can be used in different circumstances. A second objective is the performance evaluation of a vehicle based on a wedge-derived waverider forebody. The nondimensional free parameters are the angle of the wedge, the freestream Mach number, and a parameter that locates the upstream edge of the cowl. Aside from lift and drag coefficients, a number of performance parameters are derived and discussed. One conclusion is that the vehicle's performance favors a cowl lip location close to the bow shock.

6. G. Emanuel, "Shock Waves with Sweep." This work is currently being prepared for journal publication.

REFERENCES

1. Rasmussen, M.L. and He, X., "Analysis of Cone-Derived Waveriders by Hypersonic Small-Disturbance Theory," 1st International Hypersonic Waverider Symposium, University of Maryland, College Park, MD, October 17-19, 1990.

2. Yoon, Bok-Hyun and Rasmussen, M.L., "Computational Analysis of Hypersonic Flows Past Elliptic-Cone Waveriders," AME Research Report No. OU-AME-91-2, January 1991.

3. Cole, J.D. and Zien, T.F., "A Class of Three-Dimensional Optimum Wings," AIAA Journal, 7, pp. 264-271, 1969.

4. Corda, S. and Anderson, J.D., "Viscous Optimized Hypersonic Waveriders Designed from Axisymmetric Flow Fields," AIAA Paper No. 88-0369, presented at the AIAA 26th Aerospace Sciences Meeting, Reno, NV, January 11-14, 1988.

5. Rasmussen, M.L. and Clement, L.W., "Cone-Derived Waveriders with Longitudinal Curvature," Journal of Spacecraft and Rockets, 23(5), pp. 461-469, Sept-Oct. 1986.

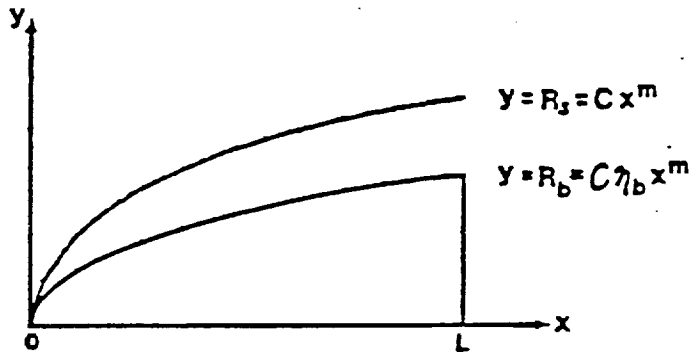

FIG. 1: Power-Law Shock and Power-Law Body

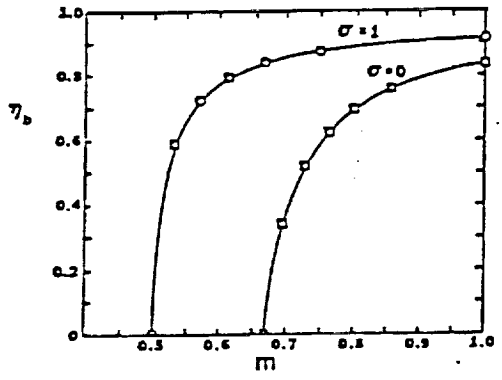

FIG. 2: Ratio of Body Radius to Shock Radius as a Function of the Index m

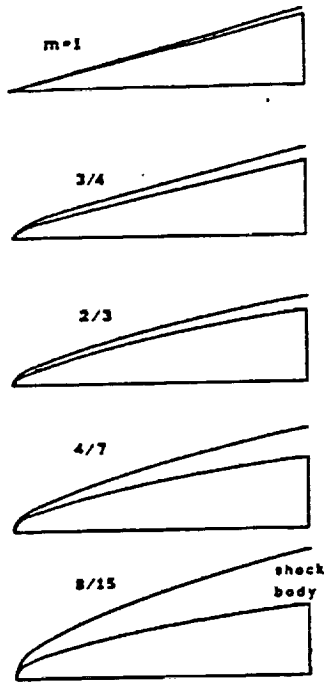

FIG. 3: Relative Shock and Body Positions for Different Values of the Power-Law Index m

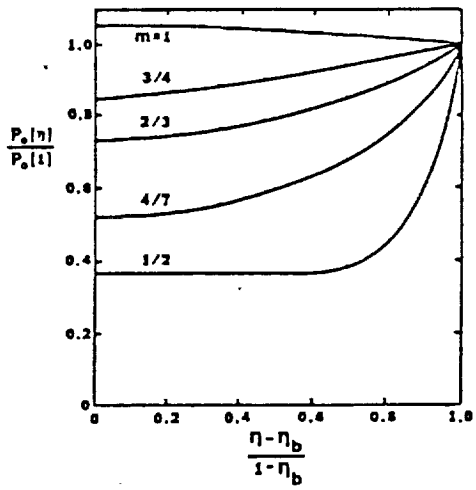

FIG. 4a: Pressure

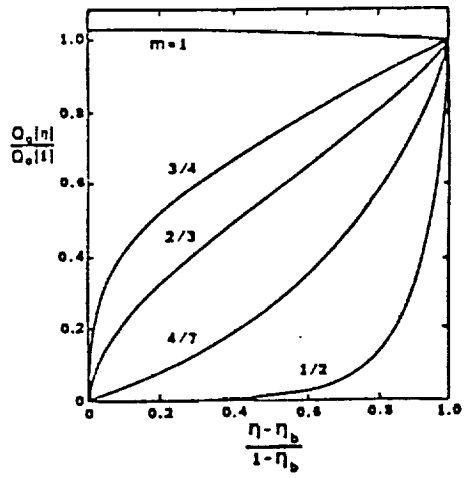

FIG. 4b: Density

Distribution of Pressure and Density Across the Shock Layer

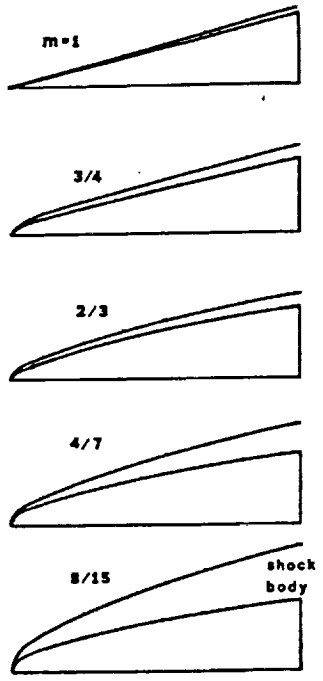

FIG. 3: Relative Shock and Body Positions for Different Values of the Power-Law Index m

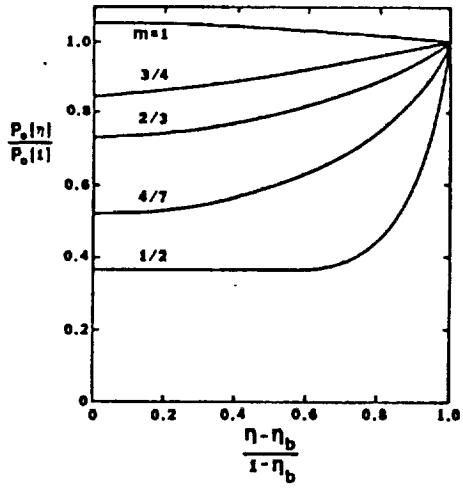

FIG. 4a: Pressure

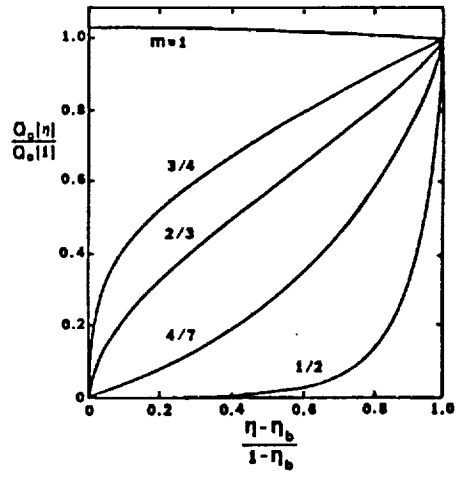

FIG. 4b: Density

Distribution of Pressure and Density Across the Shock Layer

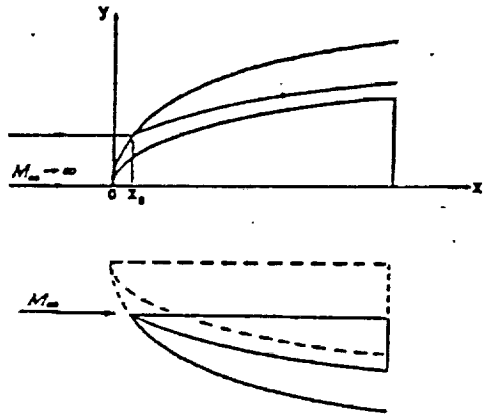

FIG. 5: Development of Waverider Longitudinal Cross-Section Shape for Power-Law Bodies

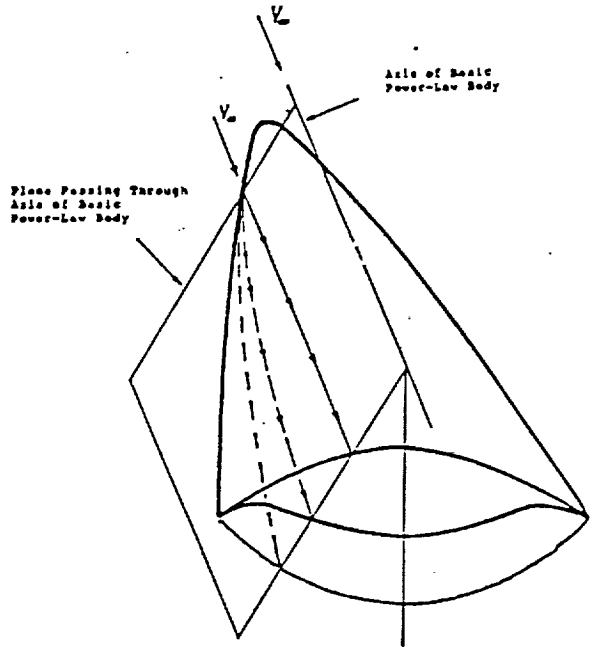

FIG. 6: Perspective of Power-Law Derived Waverider Showing Freestream and Compression-Surface Streamlines

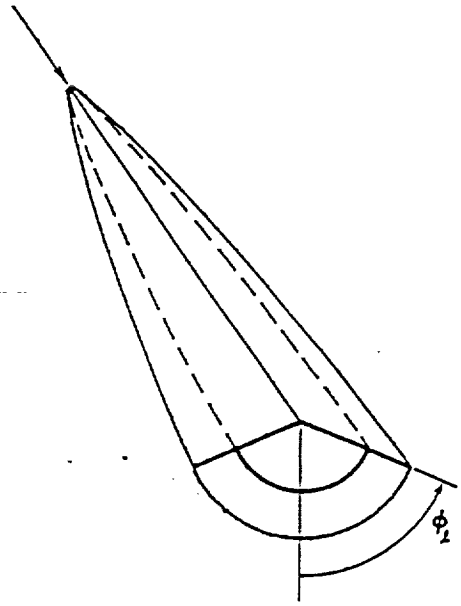

FIG. 7: Idealized Power-Law Derived Waverider

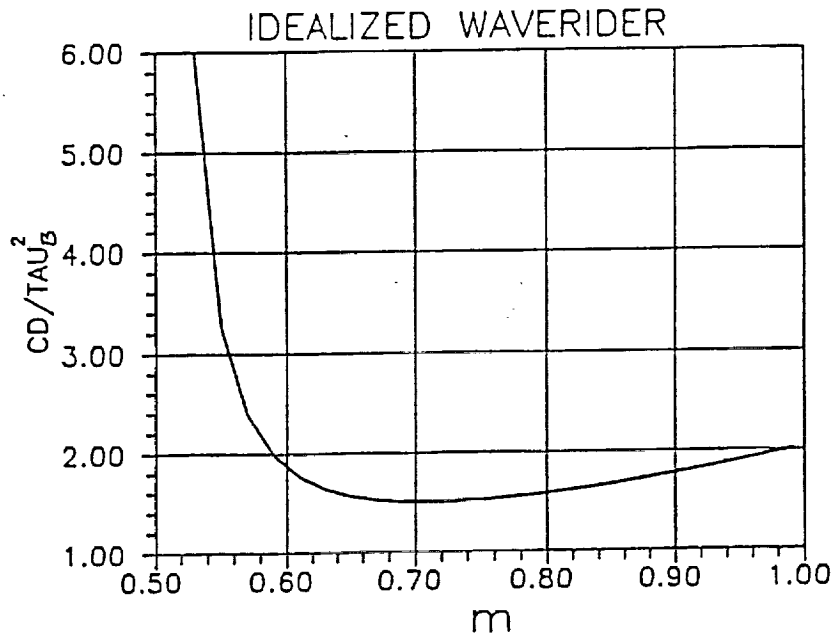

FIG. 8a: Idealized Waverider
C_D/τ_b^2 vs m

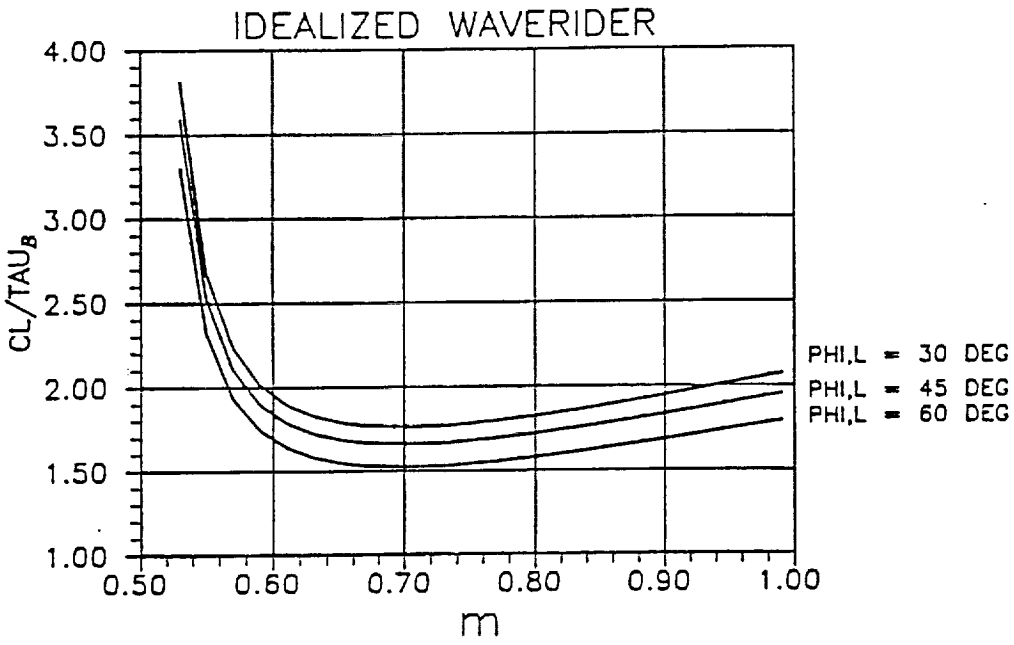

FIG. 8b: Idealized Waverider
C_L/τ_b vs m

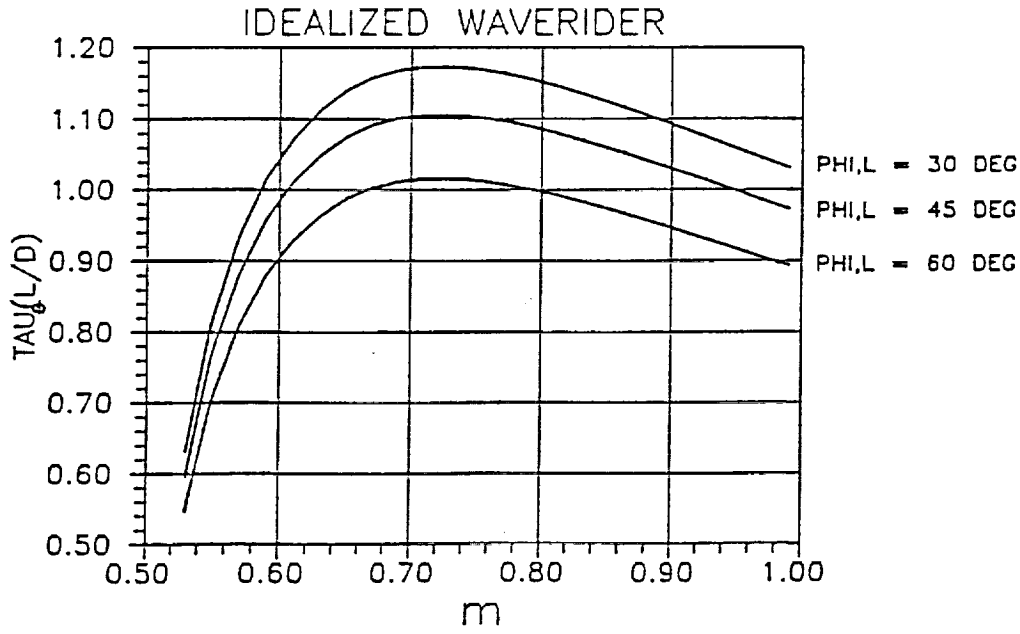

FIG. 8c: Idealized Waverider
τ_b L/D vs m

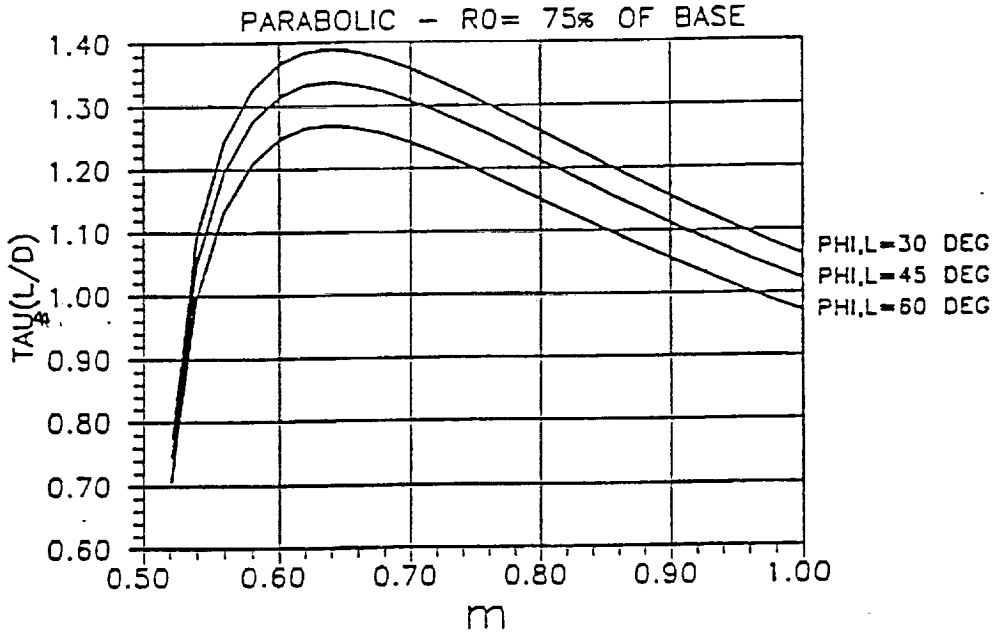

FIG. 9: Lift-to-Drag Ratio for Parabolic-Top Waverider for Various Anhedral Angles

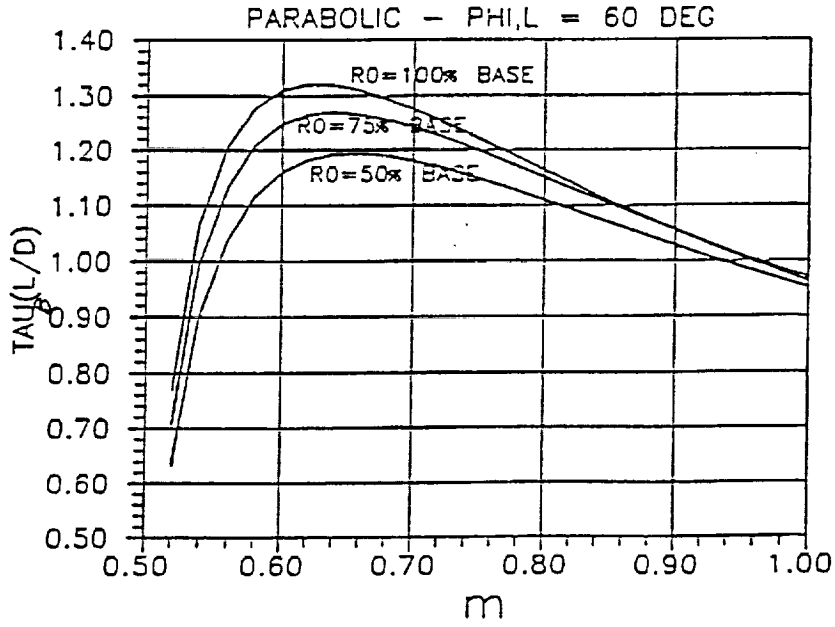

FIG. 10: Lift-to-Drag Ratio for Parabolic-Top Waverider for Various Values of R_0

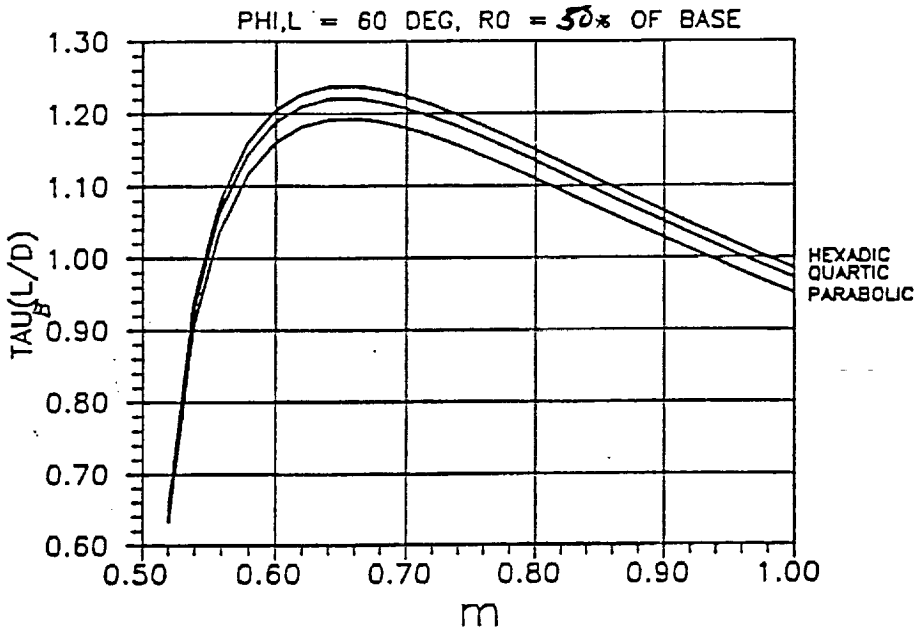

FIG. 11: Lift-to-Drag Ratio for Waveriders with Parabolic, Quartic, and Hexadic Tops